



The communication and stability evaluation of amphibious spherical robots

Liang Zheng^{1,2,3} · Shuxiang Guo^{4,5} · Shuoxin Gu¹

Received: 21 July 2018 / Accepted: 9 November 2018 / Published online: 8 December 2018
© Springer-Verlag GmbH Germany, part of Springer Nature 2018

Abstract

This paper aims to improve the collaboration ability and stability of amphibious spherical robots (ASRs). According to our previous researches, robots have no communication or control stability module. This study designed a new torque gyro control stability and an artificial electronic communication module devoted to allowing the robot to both move on land and underwater, which used a gyro sensor to design a closed-loop control module to perform terrestrial locomotion efficiently. Regarding the spherical robot mechanical structure and dynamic model, the robot communication module is designed, and the physical robot is set up to complete specific experiments. In addition, it is necessary to analyze the underwater and land motion to evaluate the performance of the robot stability motion and communication module, which includes the gait stability and velocity, and predicts the effects of the key parameters, such as electrode distance and emitter current of the amphibious spherical robot when it moves in underwater or on land. We also characterize communicate performance of the robots in still water with obstacles and natural water conditions.

1 Introduction

Nature is wonderful and can provide considerable inspiration for many robot designs, so an increasing number of biomimetic machines have appeared to carry out tasks such as underwater patrol, explorations and aquatic monitoring, which can benefit the development of the amphibious robotics technology field. Many studies on robots are based on ideas of biological systems, such as fishes, snakes, crabs, whales, turtles and other reference animals, which have shown better characteristics for adapting to

underwater, terrestrial, and aerial environments. In our previous researches about amphibious robots, we designed an amphibious spherical robot that used a multiangle rotation mode with articulated legs to move on land, flat terrain and underwater (Lin and Guo 2012; Li et al. 2017b). However, the method of this design has many limitations regarding the movement speed and stability, and the most important aspect is that the robots cannot communicate with each other or perform self-regulating stability. Our team's previously designed amphibious spherical robot was composed of a sealed transparent upper hemispheroid (234 mm in diameter) and two transparent quarter spherical shells (250 mm in diameter) that can be opened and closed (Guo et al. 2012a; Li et al. 2017a), the main reason for the two differently sized regions is that the lower hemisphere can be opened and closed quickly using two servo motors, as shown in Fig. 1, this robot has four legs, two in front and two in the rear, similar to that of a tetrapod, and has walking motion and water-jet motion, all the legs have a braking and water-jet propeller mechanism system so that the robot can move in terrestrial and aquatic environments. The entire system has ten servo motors and four water jet motors. Among them, four servo motors are used to control the horizontal direction of the legs, which are fixed on the middle tray, and the other four motors control the vertical direction of the legs. The last two

✉ Shuxiang Guo
guo@eng.kagawa-u.ac.jp

¹ Graduate School of Engineering, Kagawa University, Takamatsu, Kagawa, Japan

² Jilin Agricultural Science and Technology University, Jilin, Jilin, China

³ Changchun University of Science and Technology, Changchun, Jilin, China

⁴ Key Laboratory of Convergence Medical Engineering System and Healthcare Technology, The Ministry of Industry and Information Technology, School of Life Science and Technology, Beijing Institute of Technology, Beijing, China

⁵ Department of Intelligent Mechanical Systems Engineering, Kagawa University, Takamatsu, Kagawa, Japan

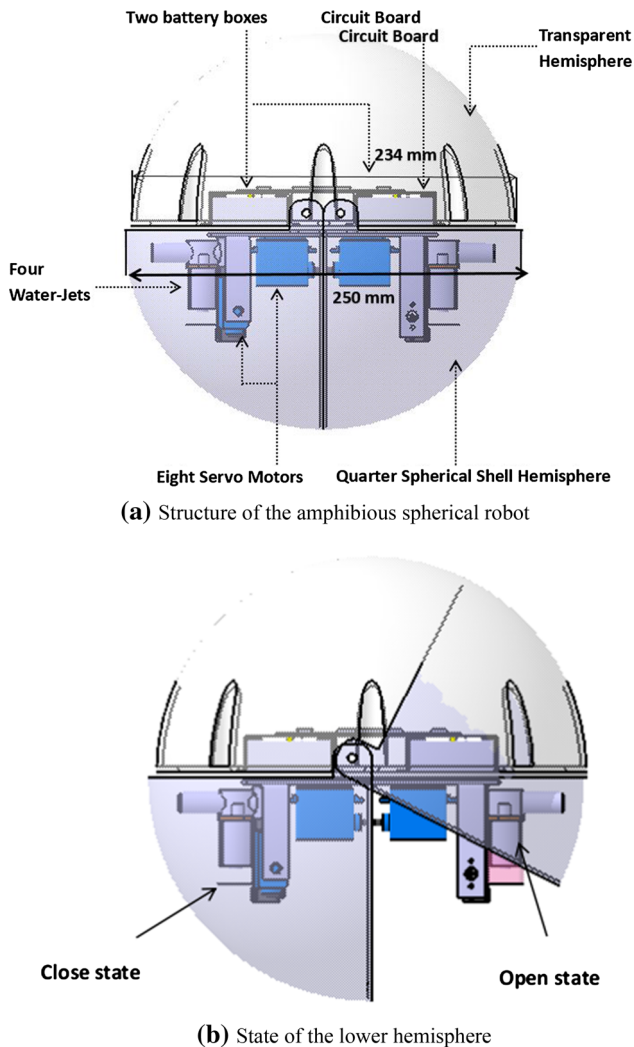


Fig. 1 Design of previous amphibious robot (Li and Guo 2016)

motors control the opening and closing of the lower hemisphere. The remaining four motors are water jet motors (Guo et al. 2017a; He et al. 2016).

Although this robot has a stable mechanical structure that can move on land and underwater freely, the electronic control system is not sufficiently advanced since this robot does not have automatic control stability or communication modules. However, some similar research has been done in terms of communication and stability modules. The stability is only a simple measurement of the angle without measuring the angular velocity and acceleration parameters. An unsolved stability problem means that the robot cannot finish complicated tasks, regardless of being on land or underwater (Guo et al. 2017b; Yue et al. 2015). The electronic control system is only based on a primary atmega2560(AVR) micro-controller, more importantly, the AVR has a low performance and low-efficiency processing speed, because the 8-bit AVR-based microprocessor combines 256 kB ISP flash memory, which is not sufficient to

meet the advanced electronic control needs, especially when dealing with communications and image data (Shi et al. 2013). This AVR micro-controller model has only dealt with some uncomplicated digital signals. Some complex signals, such as video, cannot be processed in real time. Therefore, it is necessary to use a more advanced micro-controller so that more information can be stored in this memory and the system can deal with more digital signals (Guo et al. 2017c). In addition, upgrading the data processor platform is essential. Finally, there are no automatic control balancing functions or communication modules carried on the amphibious spherical robot for terrestrial and underwater operations.

To overcome the limitations of the previous amphibious spherical robots, the main purpose of this study objective focuses on the design and development of a new type of spherical amphibious robot that contains a stability module for the control and communication module. We designed the mechanical structure of the spherical robot and performed simulation analyses according to the robot motion principle. Finally, we also simplified the performing system and decoupled the data analysis as the theoretical basis of the robot stability and communication module design.

The rest of this paper is organized as follows. In Sect. 2, we describe the general design of the amphibious spherical quadruped robot. In Sect. 3, we introduce the gyro-based automatic stability module, communication module and conduct numbers of performance test analyses, underwater exercise morphology and velocity field tests. In Sect. 4, we show the most important field tests and related discussion about the communication module and present some tests concerning the underwater communication distance experiments. Finally, in Sect. 5, the paper concludes by discussing the result and suggesting directions for future research.

2 Total structure of the amphibious robot

2.1 Structure and mechanical design

The structure of the amphibious robot is composed of two parts that contain a sealed transparent upper hemisphere and two transparent quarter spherical shells, and the shells can be opened and closed through the main circuit board by sending a digital signal to control a servomotor (Guo et al. 2017a), as shown in Fig. 2, a plastic plate is located between the upper hemisphere and lower hemisphere to carry the circuit board, the four actuating legs units and the battery installed on the plate. Controlling the servomotors allows the two transparent quarter spherical shells to open and close by rotating at an angle of 90° (Yue et al. 2013).

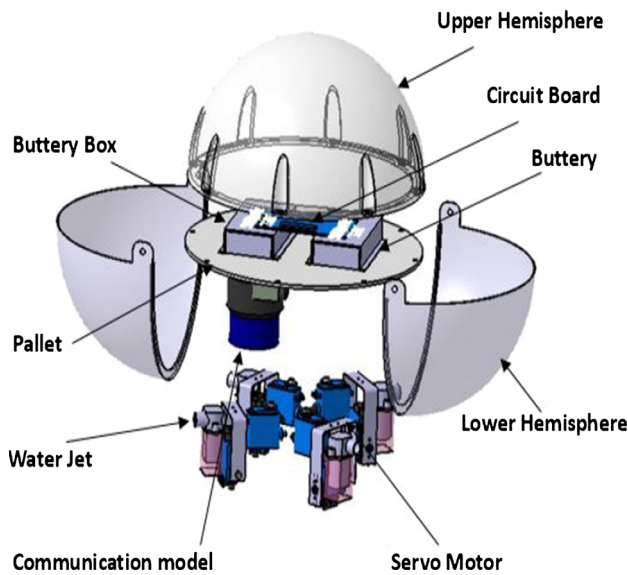


Fig. 2 The structure of the new spherical amphibious robot

Compared with other underwater robot types, amphibious spherical robots have the ability to move from the water to the ground without man power, and vice versa (Xing et al. 2018). Four-legged robots always have good performance on even ground. As shown in Fig. 3, this robot has two actuating modes: quadruped walking and water-jet propulsion, which can interconvert. The robot has four actuating legs units, each leg is composed of two servomotors and a water-jet motor, and they are symmetrically installed under the lower hull (He et al. 2015; Guo et al. 2012b). The control circuit system, sensors and power supply are installed in the upper sealed upper hemisphere. When the robot operates in the underwater mode, the lower hull closes, and the four water jets motors in the actuating units provide a vectored thrust through the strip-type holes in the lower hull to realize motion with six degrees of freedom (DOF). When the robot is in land mode, the lower hull opens, and the actuating units stretch out to walk quadrupedally under the driving force of eight servomotors (Gu and Guo 2017; Guo et al. 2017b).

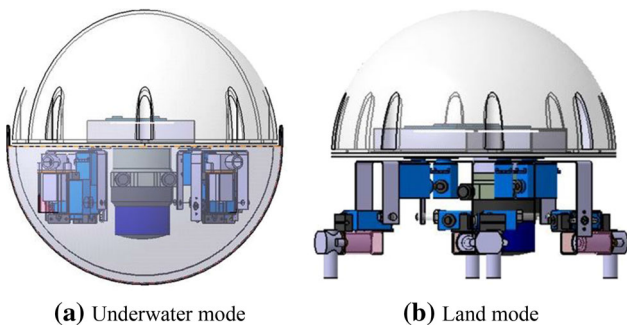


Fig. 3 Two movement modes of the spherical amphibious robot

In this design, there is a stability and communication modules installed on the center of the circuit board of the amphibious robot to measure the yaw angle to control the moving direction and transfer data information. As shown in Fig. 3, while walking, when the gyro detects a yaw angle beyond 5°, the robot is set to change its motion from walking to rotating the servomotor to stabilize the body. The amphibious robot has the ability to maintain a better dynamic performance regarding the versatility and stabilization of its direction than that of other robots. Therefore, we can use an advanced electronic control system to realize the data acquisition and stability control functions. Adding new functionality from the stability, which contains the gyro algorithm, allows the robot to automatically adjust its angle and speed through the eight servomotors. We also analyze the communication module, which installed under the middle plate, as shown in Fig. 4, the communication module of the robot is installed under the intermediate plate, because the communication module must be contact with water to achieve the purpose of underwater communication experiments. By way of doing some experimental evaluation to prove the robot better coordination achievements.

2.2 Control system modeling

Due to the limited volume, the Advanced RISC Machines (ARM) is selected as the main controller. Since the ARM has 32 PWM signals, it can connect 16 servo motors to control the arms of the amphibious robot (Lin et al. 2013; Ferrero et al. 2017). The ARM processor has a 200 MHz processing speed, which can enable real-time control of the system, and we also used the arduino controller as an information acquisition module.

To improve the efficiency of the control system for the amphibious spherical robot, we divided the total system into four parts: water-jets, servo motors, power supply and

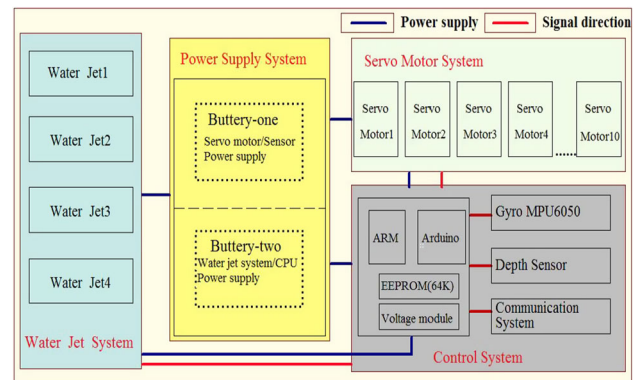


Fig. 4 The electronic control system of the amphibious spherical robot

the essential control system, as shown in Fig. 4, through the control of the servo motor, we can realize control of different motion angles (Guo et al. 2017d; Pan et al. 2015). Due to the large number of system servo motors and the fact that the system is connected to many sensors, such as water jets and electronic control circuits, the system requires a stable and increased energy storage power supply module. Hence, we designed a dual 8.4 V battery group: the “battery-one” group powered the water jet module and servo motor module, and the “battery-two” group powered the control, communication, and stability control modules. To isolate the power and control modules, the circuit control board cannot allow them to use a common ground. We use the power ground and digital ground to isolate the different signals, the control system also connected three parts: a gyro sensor, depth sensor and communication module. The ARM uses the serial RS232 bus to communicate with the gyro sensors, which control the stability of the amphibious robot when on land and underwater. The depth sensor can sense the coordinates of the underwater robot movements so that the amphibious robot can perform corresponding feedback according to the distance from the bottom of the water. The communication module enables multiple robots to communicate and transfer data with each other. This technology can lay a solid theoretical foundation for future research regarding spherical amphibious robots to realize multi-communication and cooperation.

3 Stability and communication unit

3.1 Characteristics of the control unit

The structure of the communication module (Fig. 5), due to size constraints of the robot and robot stability considerations, the sonar sensor can only be positioned as so to not interfere with the placement of other modules. This positioning does not obstruct the servo motors placement. Using 3D printed technology involves the fixed mounting of the trays with the communication sensors.

Considering that the upper hemisphere space and the gyroscope sensor position must installed at the center of the plate as much as possible, the installation position directly affects the accuracy of the stability. Therefore, the gyroscope installed in a symmetrical position between the two batteries to get the higher accuracy of the displacement parameters.

Figure 6 shows that the design uses a high-precision gyro accelerator MPU6050 connected to the main control processor through the I²C bus. The x-axis, y-axis, and z-axis angles are measured by integrating the internal pose calculator and the dynamic Kalman filter algorithm. At the

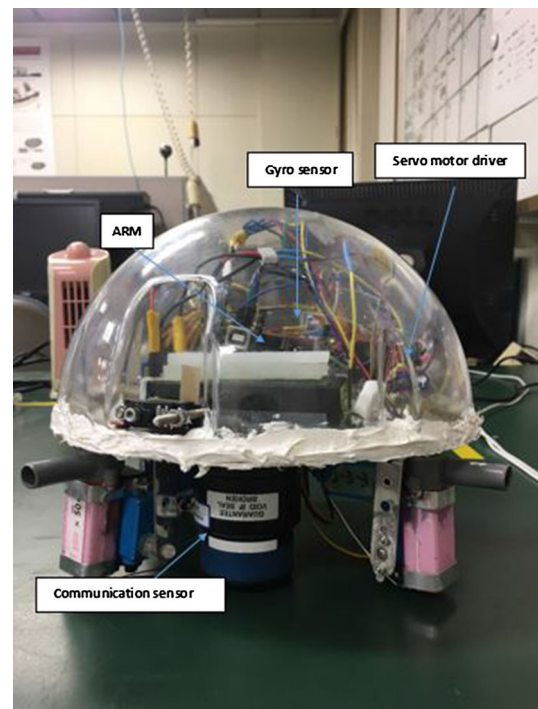


Fig. 5 The Structure of control system for ASR

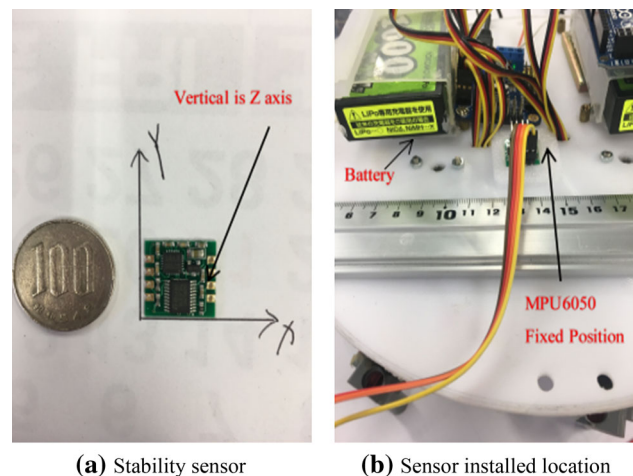


Fig. 6 Stability control board and location

same time, the power supply voltage regulator circuit is designed to be compatible with both 8 V and 5 V, and advanced digital filtering techniques are used to effectively reduce the noise that is generated in the measurement process (Wu et al. 2017). The acceleration, angular velocity, and angle directions can be measured under the dynamic conditions of robot movement. The angle output module and attitude measurement module have a good stability quality with an accuracy of 0.05°. This design method does not contain a magnetic field module, and there are no digital measurements of the yaw angle, so the yaw angle is calculated through integration.

3.2 Evaluation of the communication module

Recently, there has been an increasing interest in using multiple underwater robots to work cooperatively to finish the same task. A bio-inspired underwater robot has the ability to communicate underwater for information relay, motion coordination and formation control. However, because of the special of the underwater environment, robots cannot as easy communicate underwater as they can on land. The well-established electromagnetic communication methods, such as 3G/4G and Bluetooth (Wang et al. 2017), that are widely used on land can barely work underwater. Communication in an underwater environment more often uses visible light and sonar communication. However, the optical communication is greatly affected by the transmission media and cannot be widely used in underwater robots, in addition, optical communications cannot work in unclear water due to the line-of-sight requirements while communicating.

According to the above description, this design used the Tritech International Ltd. Micron Data Modem as the communication module (Renner 2017), as shown in Fig. 7, which can transfer data acoustically through the water. The communication is point-to-point between a pair of Micron Data Modems at operational distances up to 500 m horizontally and 150 m vertically at a data rate of 40 bits per second.

The quality of acoustic data transmission in water using conventional single frequency systems suffers considerably from multipath phenomena (Ren et al. 2017). Sound transmitted from the sending modem arrives at the receiving unit via the direct path and via a series of secondary paths due to reflections from the sea surface and sea bottom. This reflection can often result in the loss or corruption of transmitted data. In addition, conventional systems have poor immunity to the continuously varying background sea noise (such as wave noise). The Tritech Spread Spectrum technology, however, does not concentrate the acoustic energy in one waveband but produces a transmission that is linearly varied between 20 kHz and 24 kHz (known as a CHIRP waveform). As shown in Fig. 8 blow, by correlating the received signals with the CHIRP waveform, it is possible to achieve superior performance in challenging multipath environments (Pavithra and Varsha 2017; Roos et al. 2018). In addition, the identification of a unique transmission signature allows the signals to be detected in extremely noisy conditions, to the extent that communication is successful even when the signal to noise ratio is as low as -6 dB. This fact means that data streams that are considerably below the background noise level can be successfully detected.

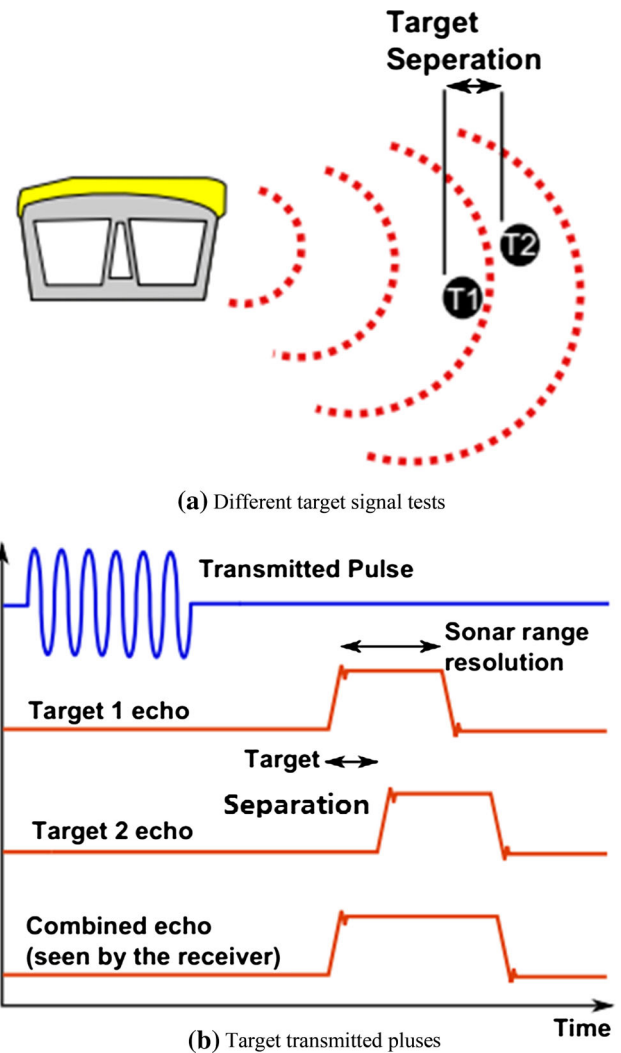


Fig. 7 **a** indicates that two targets are less than 37.5 mm apart, then they cannot be distinguished from each other. **b** indicates that the net effect is that the system will display a single large target

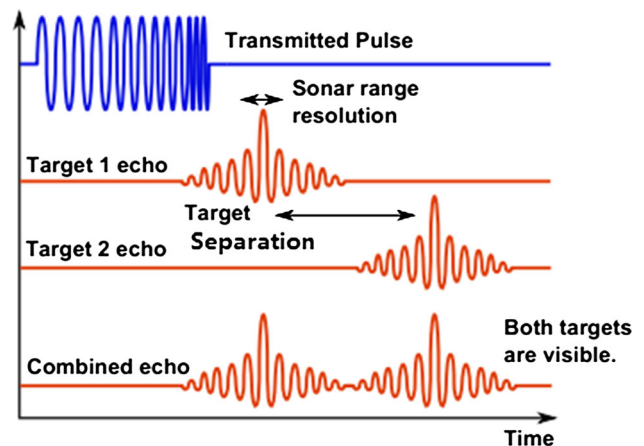


Fig. 8 The response from the pattern-matching algorithms in the sonar, the length of the acoustic pulse no longer affects the amplitude of the echo on the sonar display

As shown Fig. 8, In monotonic (single-frequency burst) sonar, the range resolution is determined by the length of the transmitted pulse. The smaller the pulse is, the greater the resolution that is achievable, and vice versa (Wang et al. 2014). The smallest pulse length is typically 50 microseconds, and the velocity of sound in water is approximately 1500 m/s, which gives a range resolution of 37.5 mm. This result effectively determines the ability to resolve separate targets (Wu et al. 2017; Ferrero et al. 2017). With the velocity of sound in water being 1500 m/s, for multiple-frequency bursts, the new range resolution is 15 mm. When two acoustic echoes overlap, the signature CHIRP pulses do not merge into a single return. The frequency at each point of the pulse is different, and the sonar is able to resolve the two targets independently.

3.3 Evaluation of the stability module

To improve the degree of intelligent control of underwater amphibious robots, we designed a closed-loop control module consisting of eight servomotors, a gyro sensor and four water-jets. The gyro accelerometer MPU6050 measures the x-, y- and z-axis angles, using the typical Kalman filter algorithm method to increase the measurement accuracy, the estimated criterion used the linear minimum, which is intrinsically different (Lin et al. 2013; Behkam and Sitti 2006). The Kalman filter has many advantages, such as good real-time performance, low memory module requirements and easy implementation of the algorithm, which is handled for univariate time-invariant systems and multivariable time-varying systems. In the gyro circuit board, we use the gyro sensor to measure the angular speed, acceleration and inclination angle. The main processor ARM controls eight servo motors and four water-jet motors by adjusting the PWM signal (Pan et al. 2015). The servo is installed in the middle of the tray between the upper hemisphere and the lower hemisphere and connected to the main controller using the signal of the gyro I²C converted to RS232. The experiment analyzed the gyro

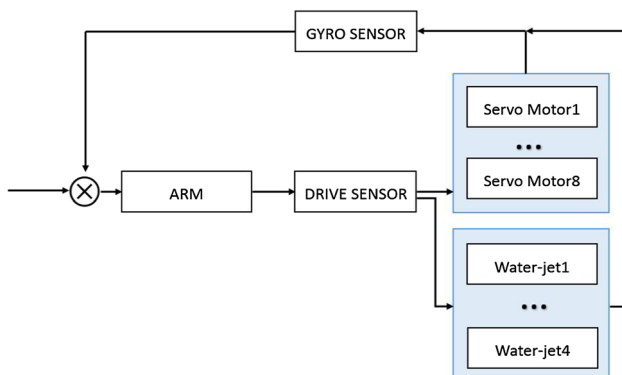


Fig. 9 Flowchart of Closed-loop control module

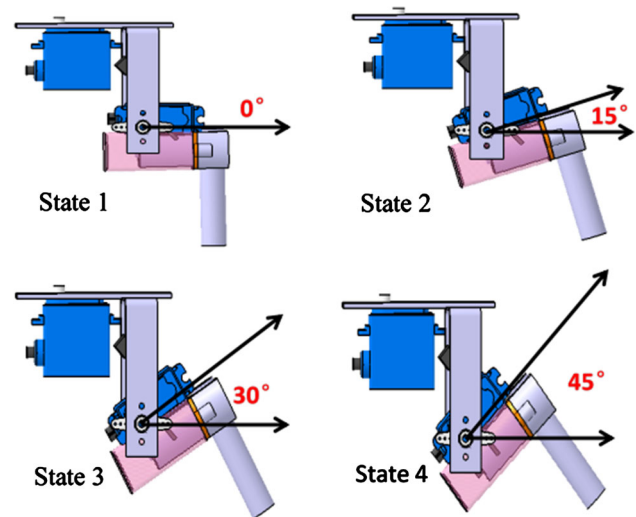


Fig. 10 Four states of the robot's legs

motion control for both land and underwater modes. The horizontal directions are the x-, y- and the z-axes, which are important parameters.

The MPU6050 is an attitude sensor that is used to obtain the tilt angles of the x-, y-, and z-axis of the object (four-axis, stability cart, angle roll, yaw angle) (Yuan et al. 2017). We read through the I²C bus of the MPU6050 six data values (triaxial acceleration AD value and three-axis angular velocity AD value) to obtain the pitch, roll, and yaw angles through the attitude fusion (Pan et al. 2011; Lin et al. 2017). Therefore, when the three angle parameters are changed, the MCU can be notified through the I²C bus to make the corresponding servomotor perform balancing actions through the PWM signal, as shown in Fig. 9.

According to the closed-loop control principle, the experiment is divided into four states of leg movement for the closed-loop control analysis. Due to the lateral limitation of the water jet motor in the leg, in the land or underwater movement modes, the maximum horizontal direction of the leg motor is 45°, and the experiments are performed under the following four states: 0°, 15°, 30°, and 45°, as shown in Fig. 10. Through the gyro sensor, according to the movement of the robot's legs, we can observe the overall acceleration and angle of the curve. The sensor then provides the corresponding PWM signal to compensate the motor sports mode so that the movement of the gyro will be back to an equilibrium status. as shown in Figs. 11–12. The red color represents the x-axis, the blue color represents the y-axis, and the green color represents the z-axis, that in addition to the momentary drift data of the angular velocity, the remainder of the plots are horizontal, indicating that the robot is in the horizontal state. Therefore, the robot does not require a PWM pulse to compensate for the x-, y- and z-axis self-stability curves

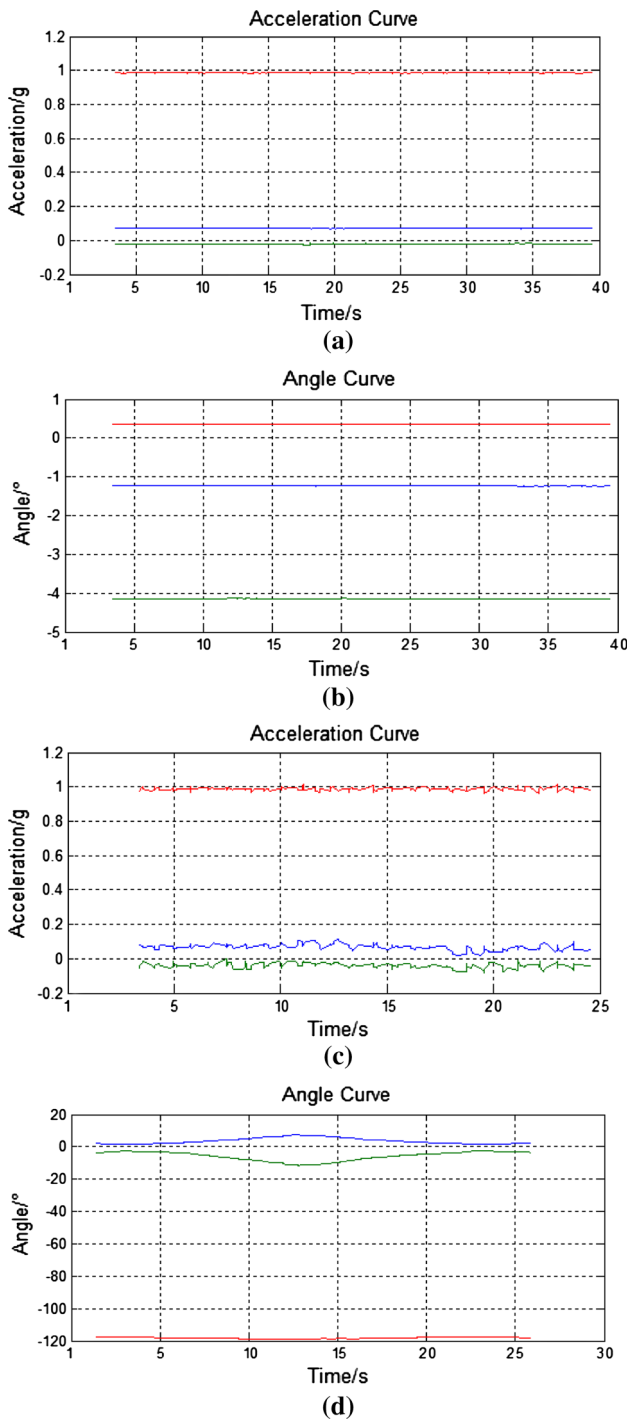


Fig. 11 Acceleration and angle curve of x-, y-, z-axis in horizontal **a**, **b** and 15° **c**, **d** state (red: x-axis, blue: y-axis, green: z-axis)

can be detected as an un-stability point and provide a PWM compensation signal.

For the four states of the robot legs, the experiment uses MATLAB to analyze the linear system of the acceleration, angular velocity and angle (Lee and Jung 2017). According to the state of the curve, the x-, y- and z-axis self-stability

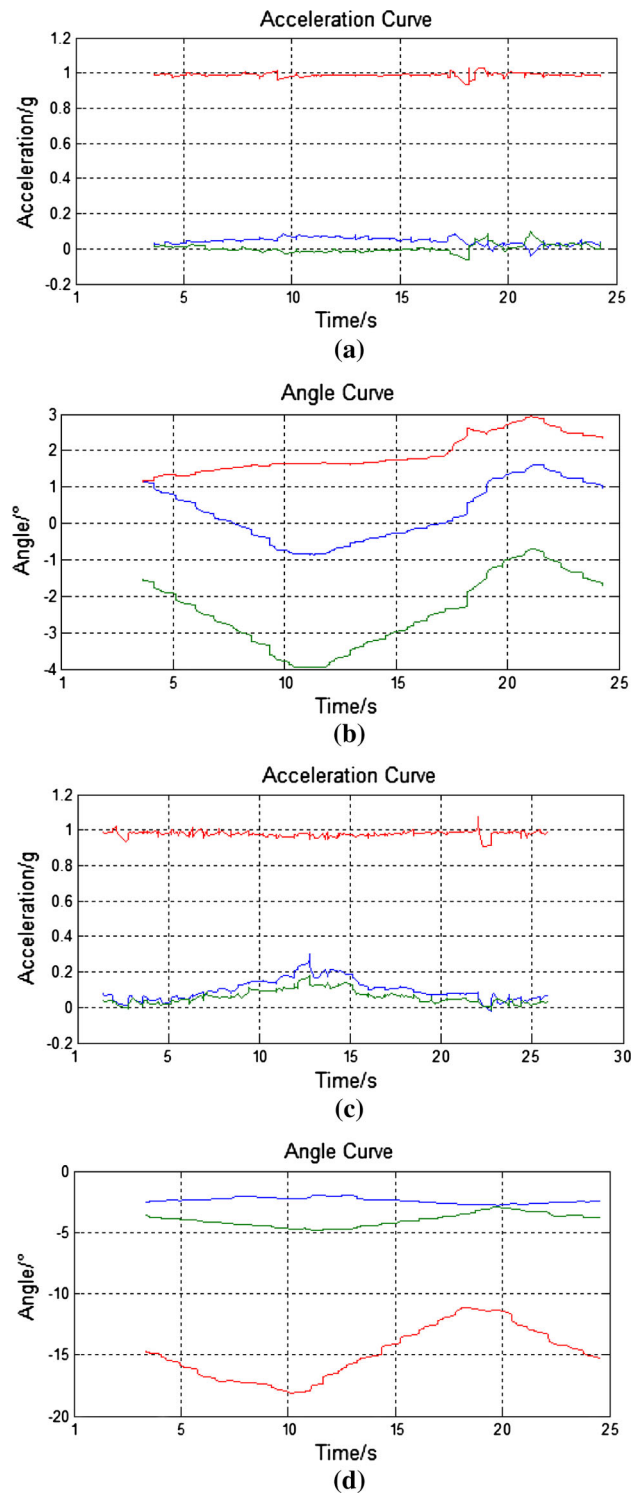


Fig. 12 Acceleration and angle curve of x-, y-, z-axis in state of 30° **a**, **b**, 45° **c**, **d** (The tilt angle of the leg) (red: x-axis, blue: y-axis, green: z-axis)

curves can be detected as an un-stability point and provide a PWM compensation signal.

Comparing the data of 0° and 15° in Fig. 11, we can be seen that the acceleration changes minimally when the leg

changes by 15° . The change of the angular velocity is relatively large, because the horizontal angle of the horizontal tray of the robot changes. The z-axis (red line) changes greatly, reaching a maximum of $10^\circ/s$. The change in z-axis angle also occurs at approximately $5^\circ/s$, so the PWM signal is required for compensation.

When the leg inclination angle reaches 45° , as shown in Fig. 12, the z-axis and y-axis accelerations change greatly, reaching almost 20° . The main reason for the change is that the tilt angle of the intermediate tray becomes larger than that of the initial state, the z-axis change tends to be flat due to the given pulse frequency. In this way, we must use the PWM to compensate. However, only the x-axes and y-axes require compensation so that the stability of the robot will not be affected. After the experiments, the PWM pulse must compensate the signals with different angles to maintain the stability of the spherical robot.

4 Experimental for characteristic evaluation

4.1 Performance of communication function

The underwater test is divided into two kinds of environments, the first test: Underwater communication distance test analysis under the environment of a square pool that is 2500 cm in length, 1500 cm in width, and 200 cm in height, the water depth is 130 cm (Fig. 13a). Second: Underwater obstacle communication test. Figure 13b shows that the communication test under the environment of a square pool that is 1100 cm in length, 600 cm in width, and 100 cm in height, the water depth is 60 cm. The time taken by the robot to move from the starting point to the end point is 206 s, the running distance is 2500 cm, and the average speed of the robot is 0.12 m/s. During the movement process, due to the participation of a stable module, the trajectory of the amphibious spherical has almost no offset.

The image acquisition points are collected at 50-s intervals to record the different states of the spherical robot movement. The main processor is connected to the communication module through the serial ports with sends seven hexadecimal digits “F” each time. The host computer records the received data, status and transmitted time. Due to distance factors, as the distance between the attached robot and the master robot (as shown in Fig. 14) is further and longer, the data received by the affiliated robot is getting longer and the bit error rate is also getting higher.

The data needs to be analyzed, the computer needs to use the serial communication mode as the collected data. Therefore, the affiliated robot does not all move underwater, and only the sonar sensor invades the underwater, so that the master robot can communicate in real time. The

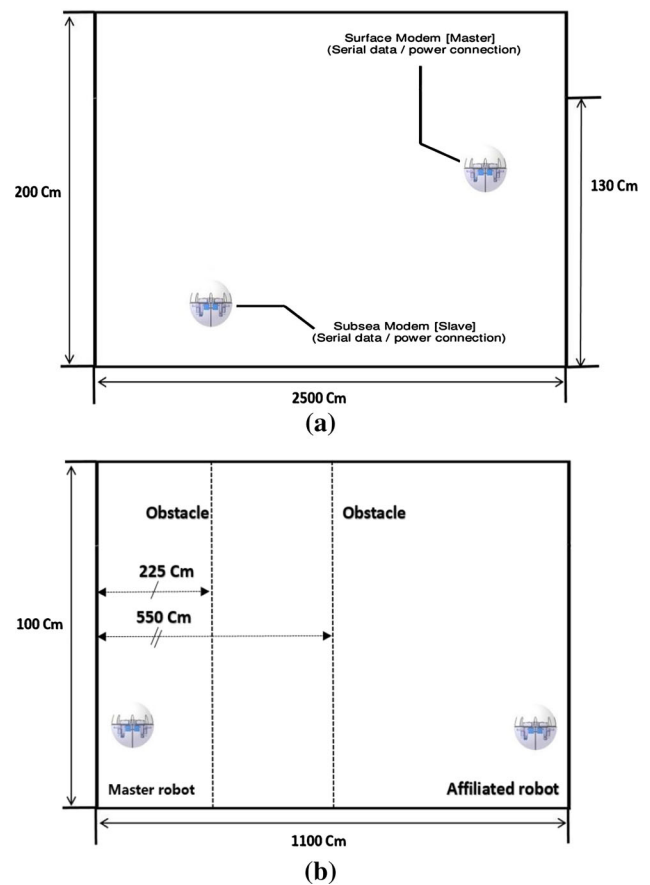


Fig. 13 Environment of underwater tests. **a** The size of underwater communication experimental site **b** Underwater communication experimental site with obstacle (obstacles are placed in two locations so that get better performance of underwater communication module)

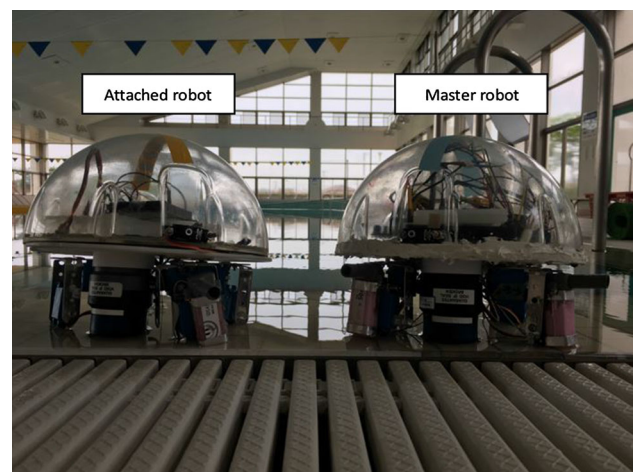


Fig. 14 Attached robot and master robot

main control circuit of the attached robot is powered by a computer, and the communication sensor is powered by an external battery (8 V, 1 A). The master robot moves into the water and moves from the starting point to the end of

the 25-m swimming pool. The computer receives the data and then performs the corresponding data analysis, as shown in Figs. 15–16.

A sound-absorbing sponge and plastic material is used as the material for isolation (Fig. 17), The master robot sends signals at different distances to the affiliated robot, and computer-controlled sonar sensors are used to read the transmitted data using the serial port. The serial monitor (0.01 accuracy) records the transmission time.

As shown in Fig. 18, the communication delay time is up to 8 s at a communication distance of 550 cm with an obstacle, and the maximum delay is 6.5 s at a communication distance of 225 cm with an obstacle, without a barrier 550 cm communication distance. The delay is only 5 s. It can be known that the influence of obstacles and communication distance in the communication module is still obvious.

4.2 Performance of stability function

The land mode experiments were carried out to evaluate the loop-control module of the amphibious spherical robot since precise position control is very important for operations and tasks both on land and underwater. Compared with the previous robot without a closed-loop control module, this design mainly tests the closed-loop control module as the robot travels along a fixed route until reaching the target. According to the changes in the angular

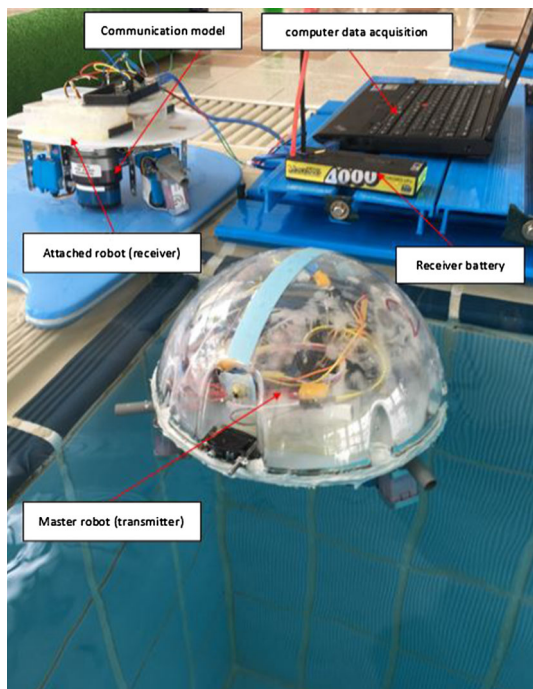


Fig. 15 Experimental set up for two robots with communication module

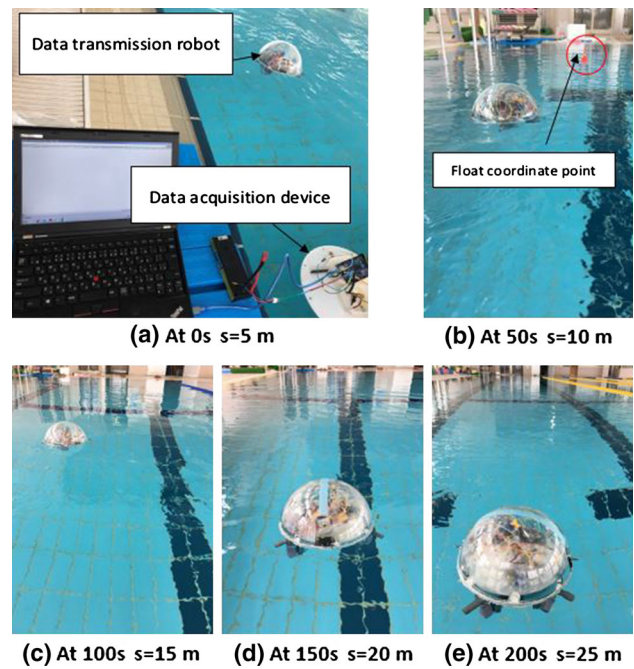


Fig. 16 Underwater experiments by different communication distance

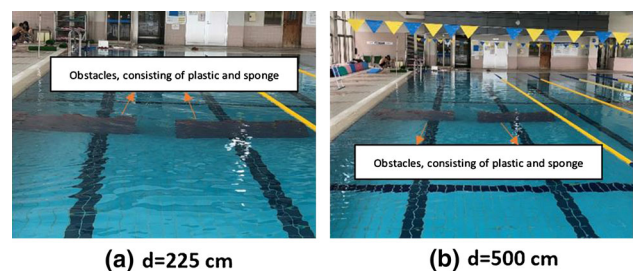


Fig. 17 Underwater experiment of different obstacle positions

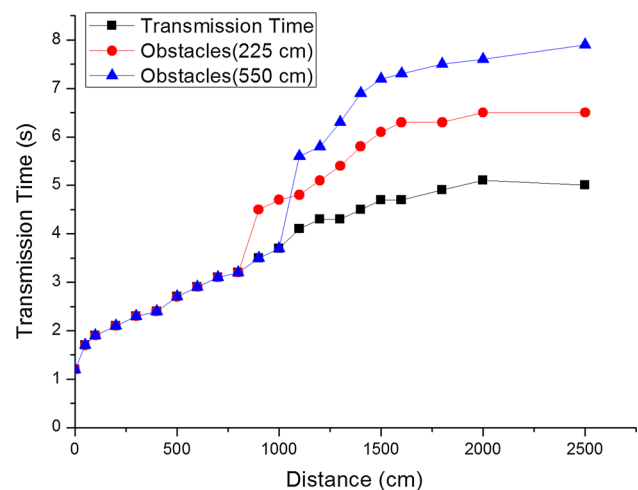


Fig. 18 Comparisons between transmission time and communication distance

speeds of the x-, y- and z-axes, the four servo motors for the land motion are controlled by the pulse width modulation method so that the robot operation is more stable and efficient.

Because the gyro sensor angular velocity accuracy is 0.6 °/s, the acceleration accuracy is 0.005 g. Therefore, the feedback angle setting of the rotation angle is very important for the closed-loop control module. The MPU6050 outputs the I²C signal and uses the I²C bus to convert the serial chip SC16IS741A into a serial port signal to facilitate use of the computer for debugging, Thus, the gyro sensor, the MPU6050, was installed on the robot to measure the yaw angle to control the moving direction when the robot operated on land. During the walking motion, when a yaw angle measured by the gyro sensor is over 5° in the x-, y- and z-axis, the loop-control module triggers control of the servo motors, which is installed on the four legs. Three axial gyro sensors can control four spray motors and eight servo motors and then decide which motors are triggered to control the robot's specified orientation.

As shown in Fig. 19, the first step is to initialize the circuit system, which can set the target of the robot and initialize the position of the servo motor, the robot starts to move, and the gyro detects the angles of the x-, y- and z-axis. The x-axis indicates lateral movement, the y-axis indicates forward movement, the z-axis indicates whether

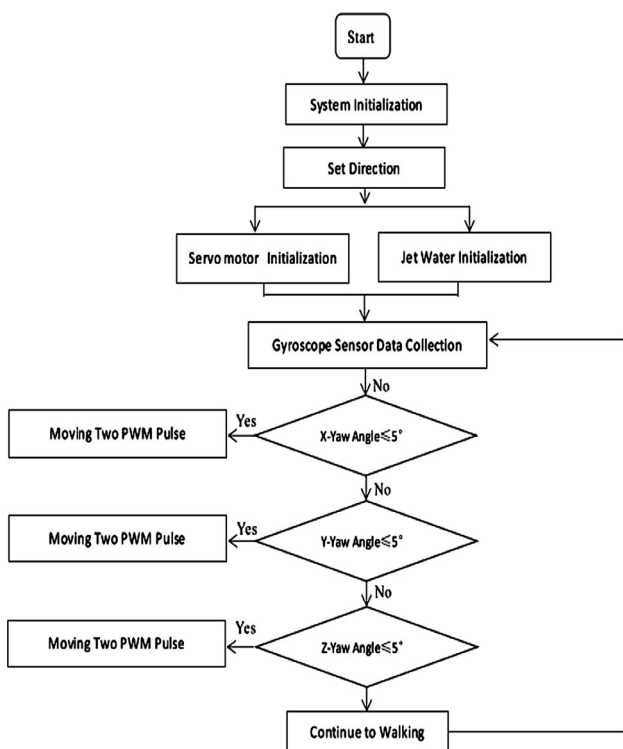


Fig. 19 Flowchart of the loop-control module

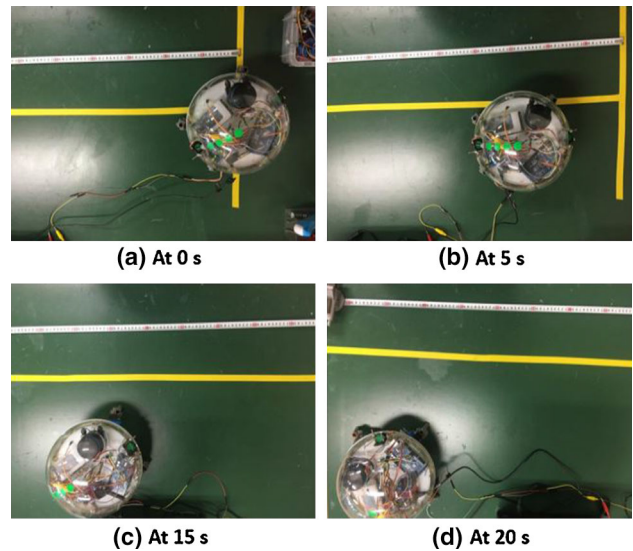


Fig. 20 Movement tests by no-gyro sensor installed

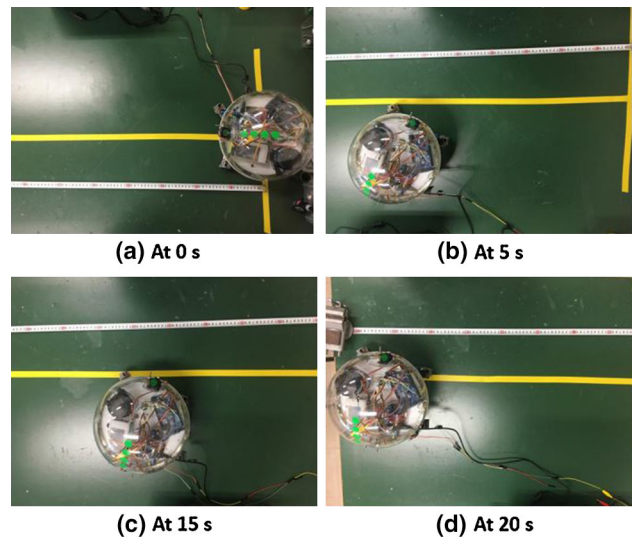


Fig. 21 Movement tests by gyro sensor installed

the robot is stability. The offset angle is greater than 5° in the land environment, so the corresponding motor is rotated. An offset angle of fewer than 5° indicates that the target is moving normally. If the sensor does not detect the three coordinate axes, the robot continues to move and feed data back to the gyro to achieve closed-loop control.

Figures 20–21 shows the testing environment is a square container that has a 135 cm length, 65 cm width, the robot moves from one side of the line to the other in 20 s. From Fig. 22, it can be clearly concluded that the red color represents a robot with a closed-loop control and that the black color represents a robot without a closed-loop control. The robot with a closed-loop module moves 143 cm in 20 s, and the robot without a closed-loop module moves

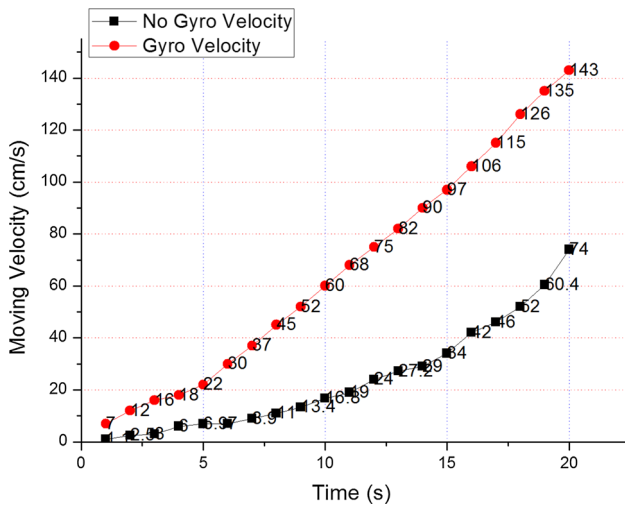


Fig. 22 Comparisons movement speed between the gyro and no-gyro module

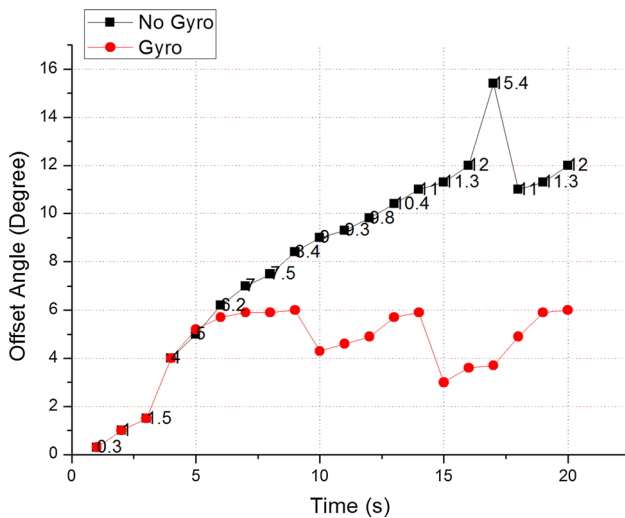


Fig. 23 Comparisons departure angle between Gyro and Non-gyro sensor

only 74 cm in 20 s (vertical distance). Therefore, a robot with a closed-loop module has twice the movement speed of a robot without a closed-loop module and is greatly improved both in terms of speed and stability.

As shown in Fig. 23, the abscissa is the moving time, and the offset angle with a closed-loop module and no closed-loop movement are analyzed within 20 s, represented by the red and black curve symbols respectively

After 20 s of movement without a closed-loop robot, the offset angle reaches 20°, but the closed-loop module robot shifts only 3° after 20 s. because the module was designed to have an offset of 5°. After the robot shifts more than 5°, after 2 s, the closed-loop module will be triggered to control the corresponding servo motor.

5 Conclusions

A novel amphibious spherical robot was developed that has a stable and efficient communication module, a control module with a better interactive system and self-regulation process than that of the previous version. First, this design uses the ARM microprocessor to be faster than the previously designed AVR processor. This processor can also provide more I/O interfaces so that the robot can add more sensors and control modules, which can improve its applicability. Second, we designed a communication module based on an industrial sonar sensor that allows the underwater robot to have the ability to communicate with multiple machines and have complete collaboration. We also use the communication module for terrestrial communication experiments, underwater communication experiments, and communication experiments with impediments underwater, giving reasonable experimental results. Third, this design contains a stable, trapped, closed-loop control module. Through the advanced gyro sensor MPU6050, three parameters of acceleration, angular velocity and rotation angle along the x-, y- and z-axes are measured. We also use the MATLAB software to analyze the two parameters under different conditions and analyze the reasons for the changes. Although the acceleration and angular velocity only a little influence in the current system, once the robot moves faster, the requirements for acceleration and angular velocity parameters increase. Fourth, at the end of the article, a detailed assessment of the entire closed-loop module was conducted in the actual external environment. The robots with closed-loop modules and those without closed-loop modules are analyzed in real time within a limited distance. Finally, we conducted several movement experiments to evaluate the performance of the directional control.

Acknowledgments This research is partly supported by National Natural Science Foundation of China (61375094).

References

Behkam B, Sitti M (2006) Design methodology for biomimetic propulsion of miniature swimming robots. *J Dyn Syst Meas Contr* 128(1):36–43

Ferrero F, Lanteri J, Brochier L et al (2017) Impact of mechanical accuracy in mmW spherical measurements. *Antenna measurements & applications (CAMA). IEEE Conf IEEE* 1(1):377–380

Gu S, Guo S (2017) Performance evaluation of a novel propulsion system for the spherical underwater robot (SURIII). *Appl Sci* 7(11):1–19

Guo S, Shi L, Xiao N, Kinji A (2012a) A biomimetic underwater microrobot with multifunctional locomotion. *Robot Auton Syst* 60(12):1472–1483

Guo S, Mao S, Shi L, Li M (2012b) Design and kinematic analysis of an amphibious spherical robot. In: 2012 IEEE international

- conference on mechatronics and automation. IEEE, 4(1):2214–2219
- Guo S, He Y, Shi L, Pan S, Tang K, Xiao R, Guo P (2017a) Modal and fatigue analysis of critical components of an amphibious spherical robot. *Microsyst Technol* 23(6):2233–2247
- Guo S, Pan S, Shi L, Guo P, He Y, Tang K (2017b) Visual detection and tracking system for a spherical amphibious robot. *Sensors* 17(4):870
- Guo J, Guo S, Li L (2017c) Design and characteristic evaluation of a novel amphibious spherical robot. *Microsyst Technol* 23(6):1999–2012
- Guo S, Pan S, Li X, Shi L, Zhang P, Guo P, He Y (2017d) A system on chip-based real-time tracking system for amphibious spherical robots. *Int J Adv Rob Syst* 14(4):1729881417716559
- He Y, Shi L, Guo S, Pan S, Wang Z (2015) Preliminary mechanical analysis of an improved amphibious spherical father robot. *Microsyst Technol* 22(8):2051–2066
- He Y, Shi L, Guo S, Pan S, Wang Z (2016) Preliminary mechanical analysis of an improved amphibious spherical father robot. *Microsyst Technol* 22(8):2051–2066
- Li Y, Guo S (2016) Communication between spherical underwater robots based on the acoustic communication methods. In: *Proceedings of the 2016 IEEE international conference on mechatronics and automation*, pp 403–408
- Lee SD, Jung S (2017) Awakening strategies from a sleeping mode to a balancing mode for a sphere robot. *Int J Control Autom Syst* 15(6):2840–2847
- Li M, Guo S, Hirata H, Ishihara H (2017a) A roller-skating/walking mode-based amphibious robot. *Robot Comput Integrated Manuf* 44(1):17–29
- Li M, Guo S, Guo J, Hirata H, Ishihara H (2017b) Development of a biomimetic underwater microrobot for a father–son robot system. *Microsyst Technol* 23(4):849–861
- Lin X, Guo S (2012) Development of a spherical underwater robot equipped with multiple vectored water-jet based thrusters. *J Intell Rob Syst* 67(3–4):307–321
- Lin X, Guo S, Yue C, Juan D (2013) 3D modelling of a vectored water jet-based multi-propeller propulsion system for a spherical underwater robot. *Int J Adv Rob Syst* 10(1):1–8
- Lin Z, Xiong Y, Dai H et al (2017) An experimental performance evaluation of the orientation accuracy of four nine-axis MEMS motion sensors enterprise systems (ES). *5th Int Conf IEEE* 2(1):185–189
- Pan Q, Guo S, Okada T (2011) A novel hybrid wireless microrobot. *Int J Mech Autom* 1(1):60–69
- Pan S, Shi L, Guo Shuxiang (2015) A kinect-based real-time compressive tracking prototype system for amphibious spherical robots. *Sensors* 15(4):8232–8252
- Pavithra D, Varsha PH (2017) A Review on underwater communication with an aerial platform. *Asian J Appl Sci Technol* 1(5):25–27
- Ren H-P, Bai C, Kong Q, Murilo SB, Grebogi. C (2017) A chaotic spread spectrum system for underwater acoustic communication. *Statistical Mech Appl* 478(3):77–92
- Renner C (2017) Packet-based ranging with a low-power, low-cost acoustic modem for micro AUVs. In: *proceedings of 11th international itg conference on systems, communications and coding*, vol 11, no 1, pp 1–6
- Roos F, Appenrodt N, Dickmann J et al (2018) Waveform multiplexing using chirp rate diversity for chirp-sequence based MIMO radar systems. *2018 IEEE radio and wireless symposium (RWS)*. Univ Ulm 10(2):60–63
- Shi L, Guo S, Mao S, Yue C, Li M, Asaka K (2013) Development of an amphibious turtle-inspired spherical mother robot. *J Bionic Eng* 10(4):446–455
- Wang K, Liu Y, Li L (2014) Visual servoing trajectory tracking of nonholonomic mobile robots without direct position measurement. *IEEE Trans Rob* 30(4):1026–1035
- Wang W, Liu J, Xie G et al (2017) A bio-inspired electrocommunication system for small underwater robots. *Bioinspiration Biomimetics* 12(3):036002
- Wu TC, Chi YC, Wang HY, Tsai CT, Lin GR (2017) Blue laser diode enables underwater communication at 12.4 Gbps. *Sci Rep* 1(7):1–9
- Xing H, Guo S, Shi L, H Y, S Su, Chen Z, Hou X (2018) Hybrid locomotion evaluation for a novel amphibious spherical robot. *Appl Sci* 8(2):156–180
- Yuan F, Wei Q, Cheng E (2017) Multiuser chirp modulation for underwater acoustic channel based on VTRM. *Int J Nav Architect Ocean Eng* 9(3):256–265
- Yue C, Guo S, Shi L (2013) Hydrodynamic analysis of the spherical underwater robot SUR-II. *Int J Adv Rob Syst* 10(5):1–12
- Yue C, Guo S, Li M, Li Y, Hirata H, Ishihara H (2015) Mechatronic system and experiments of a spherical underwater robot: SUR-II. *J Intell Rob Syst* 80(2):325–340

Publisher's Note Springer Nature remains neutral with regard to jurisdictional claims in published maps and institutional affiliations.